Merima Muslić ✉
Vera Rede
Zdenka Keran
Helena Lukšić

https://doi.org/10.21278/TOF.494079425
ISSN 1333-1124
eISSN 1849-1391

INFLUENCE OF THE EQUAL CHANNEL ANGULAR EXTRUSION ON THE ALUMINIUM-FLY ASH COMPOSITE

Summary

This paper presents the influence of equal channel angular extrusion on the microstructure and properties of composites based on the A356.0 aluminium alloy with the addition of 6 wt.% fly ash as reinforcement. The composite was produced using the compo casting method. The microstructure of the composite was analysed using an optical microscope, computer tomography, and scanning electron microscopy. Rosettes and spheroidal particles were observed in the microstructure of the cast sample, and there was a good distribution of fly ash within the matrix. Equal channel angular extrusion was performed in three passes at the same parameters. After each pass, the microstructure was refined, and fly ash was even better mixed into the matrix. Thus, the strength and hardness of the composite increased after each pass. A fully homogeneous material was achieved after the second pass.

Key words: *equal channel angular extrusion; aluminium-fly ash composite; fly ash; computer tomography; scanning electron microscopy*

1. Introduction

Metal matrix composites (MMCs) are already widely used in various industries, such as automobile, aircraft, marine, nuclear, and chemical, and in other applications. Among MMCs, aluminium-based composites play a significant role, especially in the automobile industry, where they are used to manufacture pistons, brake pads, front and rear bumpers, door panels, hoods, roof panels, insulation, instrumental panels, and other products [1–3]. Various reinforcement materials, such as silicon carbide (SiC), titanium carbide (TiC), aluminium oxide (Al_2O_3), boron carbide (B_4C), and graphite, are used to produce aluminium-based MMCs. However, each of these materials has a certain price; for example, the price of aluminium oxide is 150 USD/kg. Therefore, the latest research also focuses on using low-cost waste materials as reinforcements, such as fly ash (FA), a byproduct of coal combustion in thermal power plants [3–5].

Fly ash is a waste material collected in thermal power plants' electrical filters of exhaust gases. All around the world, these power generators produce more than 500 million tonnes of FA per year [6]. The dimensions of the FA particles are up to 120 μm, so they present a danger

to the respiratory system and a serious problem for waste management. Only 25 to 30% of this waste material is reutilised in different sectors [6,7]. Fly ash mainly consists of metal oxides, with aluminium oxide among them; this makes it appropriate for reinforcing aluminium-based composites [5,8].

There are different methods for producing aluminium-fly ash composites, and the most common is stir casting. This method consists in adding fly ash in powder state to the molten aluminium matrix by stirring. There are different designs of furnaces and equipment for several techniques that use the same principle [9].

When it comes to solidification, aluminium-based materials can create an inhomogeneous, dendritic microstructure with coarse crystal grains. Rheological processing, which involves stirring in a semi-solid state, is performed to prevent dendrite growth and improve the microstructure. When a reinforcement material is mixed into a semi-solid matrix during the composite manufacturing process, the process is called compo casting [10–13].

By adding a reinforcement material to the metal matrix, the properties of the base material can be improved. Small particles of reinforcement material mixed in the matrix will prevent the growth of crystal grains, and if nano-fine particles are involved, they can interrupt the movement of dislocations. This means that they behave like precipitates. The strengthening of the material, i.e., the presence of a fine phase in the microstructure, is known in the literature as the Hall-Petch effect [14,15].

The Hall-Petch effect can also be achieved by refining the microstructure through severe plastic deformation (SPD). As a scientific concept, SPD is based on the work of the Nobel Prize winner P.W. Bridgeman, who studied phase transformations of materials that occur under extreme conditions of very high pressure, temperature, and shear stress. Such conditions prevail in the Earth's crust during the formation of cores and minerals. To simulate these conditions, Bridgman developed a high-pressure torsion (HPT) method. Today, the method is still successfully used for laboratory purposes, but it has not seen industrial application. Wanting to apply the principles of the SPD metal forming process for industrial purposes, Segal developed procedures in which a simpler type of motion achieves such deformations. The method is known as equal channel angular pressing/extrusion (ECAP/ECAE), where simple sliding shear stresses are used instead of torsion to change the microstructure. The technique had been developed and optimised since the 1980s, and it eventually became the first commercially applied SPD technique [16,17]. Studies confirm that the ECAE technique results in the formation of ultrafine grains with sizes of several hundred nanometres, which leads to improvements in the hardness and mechanical resistance of aluminium-based composites [18]. Reviews published in recent decades emphasise that increasing the fly ash content in the composite up to a certain optimum level yields improved mechanical properties, while higher contents or poor dispersion may cause a degradation in performance [19].

The application of equal channel angular extrusion for the production and microstructure development of the aluminium-fly ash composite is an exciting research subject due to various combinations of aluminium-based matrix, the fly ash origin and its ratio, and the number of passes. Severe plastic deformation results in significant microstructure changes that can cause material improvement. By applying several ECAE passes, a better distribution of reinforcement material and an improvement in the properties of the composite are expected [20–23].

2. Materials and methods

A composite, based on the A356.0 aluminium alloy and reinforced with 6wt.% FA, was produced using the compo casting method. This means that the reinforcement material was added by mixing it into the semi-solid matrix [9,10]. The temperature was about 620 °C, between the liquidus and solidus lines of the phase diagram. Mixing was performed using a

rotation shaft with a paddle at 500 rpm for 5 min. After a rheological treatment, the mixture was poured into a die preheated at 600 °C and left to cool to room temperature. These parameters are optimised and described in four studies on casting listed in References [24–27].

The A356.0 aluminium alloy used as a matrix is a commercial alloy intended for the production of machine parts in the automotive and other industries. This alloy has good mechanical and technological properties, and it is used for composite production [2,11,12,28]. The composition of the specific alloy is shown in Table 1.

Table 1 *The chemical composition of the A356.0 aluminium alloy*

Element	Si	Fe	Cu	Mn	Mg	Zn	Ti	Sr	Al
wt.,%	7.0	0.11	< 0.01	< 0.01	0.37	0.01	0.12	0.056	balance

The primary alloying element in this alloy is silicon, present at a concentration of 7 wt.%. Silicon dissolves well in aluminium in lower percentages and forms an α-solid solution. The eutectic of the Al-Si alloy is about 10 wt.% Si, so this alloy is hypoeutectic. Alloying aluminium with silicon improves casting properties, and the A356.0 alloy is declared as a casting alloy. The A356.0 alloy contains a small amount of magnesium, which improves wear resistance and raises the possibility of heat strengthening in Al-Si-Mg alloys [28]. In addition, a small amount of magnesium enhances the wettability of reinforcement particles in the composite production [29]. Other elements in this composite are impurities and trace elements.

The properties and composition of fly ash largely depend on its source, more precisely on the coal used in the thermal power plant. The fly ash used in the production of the investigated composite originates from the ‘Kolubara’ thermal power plant in Veliki Crljeni, Serbia. The fly ash was previously sieved, and only a fine particle fraction was used. The dimensions of the sieve mesh were 45 μm × 45 μm. Figure 1 shows the morphological shape of the fly ash used. As one can see, the particles are of different shapes, both in the shape of regular spheres and in irregular shapes.

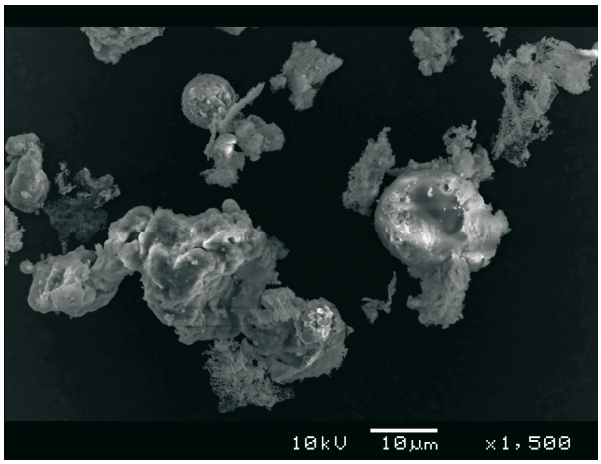

Fig. 1 A SEM image of the fine particle fraction of fly ash

The fly ash used in the composite production consists mainly of oxides, as shown in Table 2.

Table 2 *The oxide content in the fine particle fraction of fly ash*

Content	SiO_2	Al_2O_3	Fe_2O_3	TiO_2	MnO	CaO	MgO	LOI *	Total
wt.,%	37.8	22.5	17.4	0.8	0.2	12.4	3.1	1.6	95.8

* LOI – loss on ignition.

Subsequently, the cast samples were cut to dimensions of 11.8 mm × 11.8 mm × 120 mm, suitable for the two-part ECAE die with perpendicular channels, shown in Figure 2. Channels have a square cross-section with dimensions 12 mm × 12 mm.

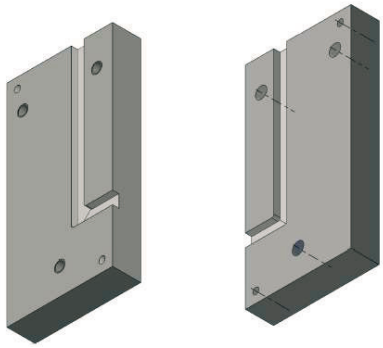

Fig. 2 A two-sided ECAE tool with a square cross-section of the channels

Extrusion was performed on a HYDRAUMA PYE40 hydraulic press (Hermann Grimm KG, Triebes, Germany) with a working force of 122 kN and a velocity of less than 0.02 m/sec. Molybdenum disulphide was used as a lubricant. The procedure was performed at room temperature. In this process, the material is compressed in the vertical channel, after which it begins to flow into the side channel. Intense shear forces cause changes in the material's microstructure. When several passes are made, it is possible to use a different orientation of the workpiece after each pass. Figure 3 shows the basic routes, while Figure 4 shows the shear planes depending on these routes. After each pass, the material was rotated around its longitudinal axis by 90°, according to the route Bc. This route causes the most significant changes, which is why it was chosen for our research [16,23,30].

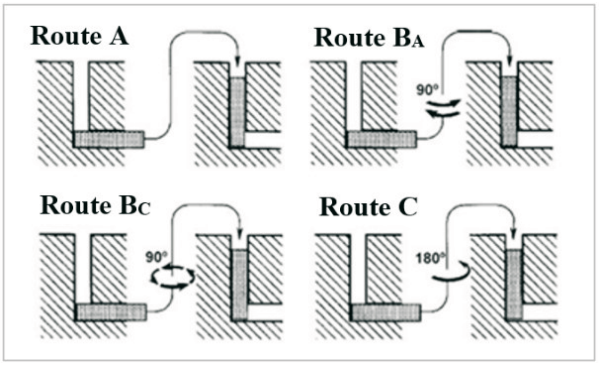

Fig. 3 Basic routes in a multi-pass ECAE [16]

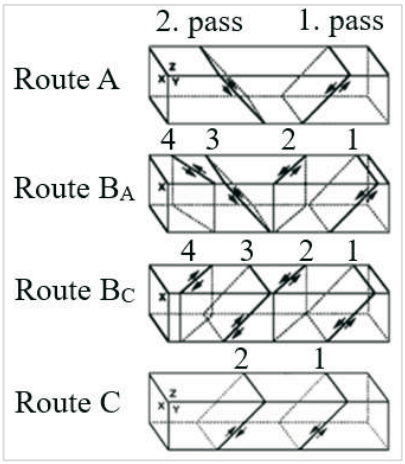

Fig. 4 Shear planes for different ECAE routes [16]

Samples for characterisation were taken after casting and after each ECAE pass. The samples were cut and metallographically prepared. Surfaces perpendicular to the extrusion direction were observed. Metallographic preparation included grinding and polishing the samples with a final abrasive grain size of 0.03 μm. If necessary, some samples were mounted in polymer mass for easier handling.

Microstructure analysis was performed by optical microscopy, computed tomography (CT), and scanning electron microscopy. Microstructure analysis was performed using an Olympus GX51 optical microscope (Olympus, Tokyo, Japan). Grain size was determined by the standard method according to ASTM E112-24 [31]. Computed tomography was performed

on a METROTOM 6 scout device (Carl Zeiss Industrielle Messtechnik, Oberkochen, Germany) in order to determine the fly ash distribution in the cast composite and the impact of plastic deformation. Computed tomography was performed with the following specific parameters: high voltage - 180 kV, power - 50 W, exposure time - 1300 ms, number of projections - 1800, and prefilter - Cu 0.5 mm. The resolution was 20 µm. Scanning microscopy was provided by a Tescan Vega TS5136MM scanning electron microscope (TESCAN, Brno, Czech Republic) with parameters visible at the bottom of the scans.

The hardness of the samples was measured using the standard Vickers method at a load of 9.81 N (HV1) using a ZHVµ-ST hardness tester (ZwickRoell, Ulm, Germany). The measurement was performed on the cross-section perpendicular to the extrusion direction. There were 12 repetitions of indentation in a duration of 10 s. The mechanical strengthening was estimated based on the Hall-Petch effect.

3. Results and discussion

In this section, we present and discuss the results of microstructure analysis, mechanical strengthening analysis related to the Hall-Pech effect, computer tomography, and the Vicker's hardness measurement.

3.1 Microstructure analysis

Figures 5–8 show all samples at a magnification of 200×, where 0 represents the cast sample, I represents the sample after one ECAE pass, II represents the sample after two passes, and III represents the sample after three ECAE passes. In all samples, a lighter area of primary α-Al crystals can be observed, which are solid solutions of silicon in aluminium. Among them is an area of eutectic. In this hypoeutectic alloy, eutectic is a mixture of primary α-Al crystal phase and silicon, excreted in the form of needles, which are visible in grey colour. The dark area is fly ash (FA).

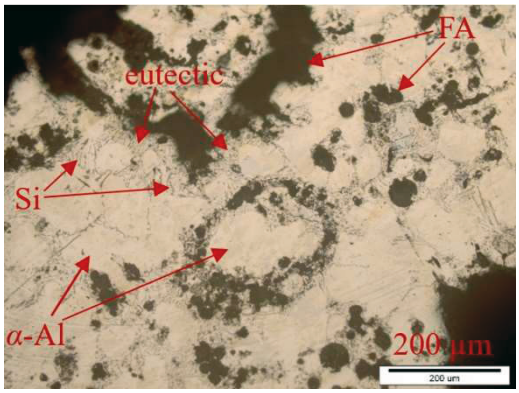

Fig. 5 Microstructure of the sample 0

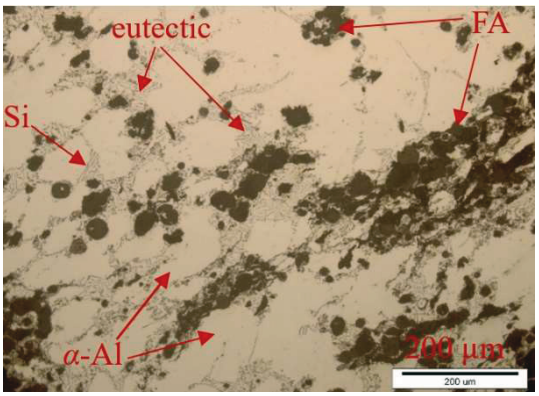

Fig. 6 Microstructure of the sample I

In the cast sample, Figure 5, the influence of semi-solid-state processing is evident. The microstructure is not a coarse-grained dendritic structure typical for aluminium cast alloys. There are mature rosettes [26,27] as well as spheroid shapes visible in the cast sample. Although the fly ash is well distributed across the cross-section of this sample, small and larger agglomerations are also visible.

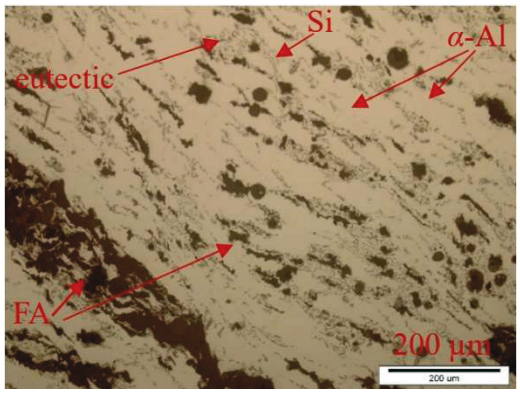

Fig. 7 Microstructure of the sample II

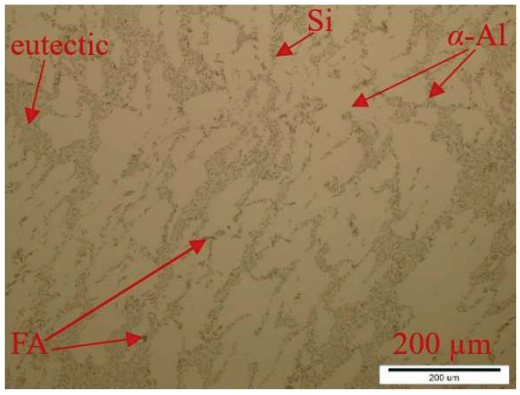

Fig. 8 Microstructure of the sample III

Figures 6–8 show the deformation of the primary crystals after each ECAE pass with respect to the cast sample structure. Figure 6 shows the microstructure of the sample after the first ECAE pass, where the ratio of length to width of the primary crystals is about 2:1. In Figure 7, after the second ECAE pass, the ratio of width to length of the grains is 4:1. The material homogenization can be observed in Figure 8. The crystal microstructure is smaller, and there are no noticeable elongations. This is a result of severe deformation caused by the Bc route previously shown in Figure 4. In the eutectic mixture, the fracture of the silicon needles can also be observed. Figure 9 shows the eutectic at 500× magnification to enable the observation of the reduction of silicon needles.

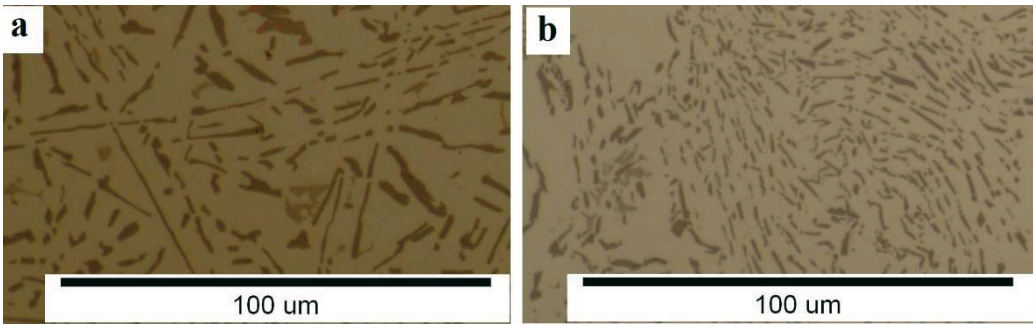

Fig. 9 Eutectic a) cast composite, b) after III ECAE passes

The fly ash was better distributed in the matrix after each ECAE pass, and the agglomerations were broken.

3.2 The Hall-Pech effect and mechanical strengthening

The Hall-Petch effect is also known as grain boundary strengthening. It is based on the principle that states that the grain boundary presents an obstacle to the movement of dislocation; thus, reducing the grain size increases strength. Up to a reduction of the grain to 20–30 nm, this effect can be described by the Hall-Petch expression [14,15]:

$$\Delta\sigma_{HP} = k \cdot (d_1^{-1/2} - d_0^{-1/2}), \tag{1}$$

where $\Delta\sigma_{HP}$ is the yield strengthening, k is the constant that depends on the material, and d_1 and d_0 are the start and finish average grain diameters.

Table 3 shows the average grain diameters of all samples:

Table 3 *Average grain diameters of the primary crystals according to ASTM E112-24*

Sample	0	I	II	III
Average grain diameters, mm	0.130 – 0.090	0.065 – 0.045	0.045 – 0.030	0.045 – 0.030

For the aluminium alloys with yield strength of about 200 MPa, k is 0.14 MPa·m$^{1/2}$ [14]; the strength values due to ECAE can be determined according to expression (1) as follows:

$\Delta\sigma_{HP\ 0\text{-}I}$ = 2.61 – 8.59 MPa – The increase in strength between the samples 0 and I

$\Delta\sigma_{HP\ I\text{-}II}$ = 0.00 – 8.20 MPa – The increase in strength between the samples I and II

$\Delta\sigma_{HP\ II\text{-}III}$ = 0.00 – 4.69 MPa – The increase in strength between the samples II and III.

Generally, the increase in yield strength between the cast sample and the sample after three passes of extrusion is:

$\Delta\sigma_{HP\ 0\text{-}III}$ = 6.11 – 13.28 MPa.

If the yield strength of the commercial A356.0 cast alloy of 190 MPa is taken as a reference value [32], the strength increase between the as-cast and triple-extruded states can be estimated at 3.2–7.0%. Although the grain boundary of the second phase of the alloy (eutectic) could not be determined, it was observed that the silicon needles after extrusion are smaller, which may also affect the prevention of dislocation movement and the increase in strength of the material. Similarly, fly ash particles in the microstructure may also contribute to the increase in strength due to the Hall-Petch effect; therefore, the gained values are a minimum strength increase.

3.3 Computer tomography

Computed tomography (CT) was performed on all samples in several different planes, but due to a limited space, only representative images are shown in Figures 10-13. Notice that the mesh dimensions in the background are 1mm × 1 mm. Industrial CT uses X-rays that pass through the examined object and end on a detector. Depending on the density of the material, the X-rays are attenuated. Based on the received rays, the detector creates images in shades of grey. Less dense materials are darker in colour.

Figure 9 shows a CT scan of the cast composite in the horizontal plane (H) in the middle of the material, which is shown by a small image in the upper left corner. In Figure 10, the same sample is shown, but a CT scan is taken in a vertical (V) section. Lighter areas correspond to the matrix (A356.0 alloy), and darker grey areas are fly ash. One can notice that there is a good distribution of fly ash in both sections. Some black areas correspond to the empty space or air, which are pores.

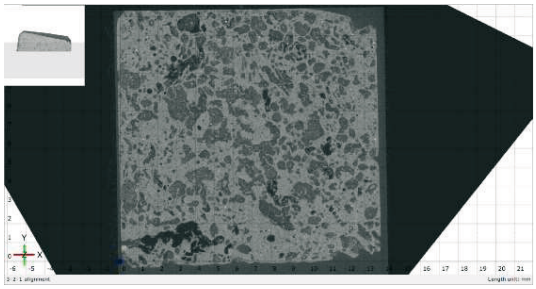

Fig. 10 A CT scan of the sample 0 in the H plane

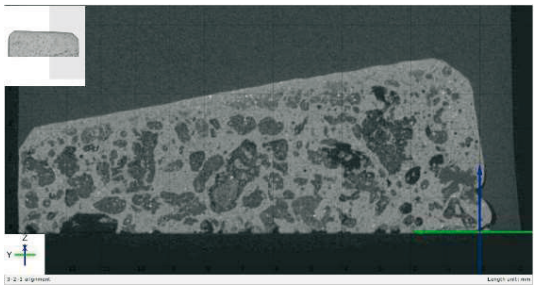

Fig. 11 A CT scan of the sample 0 in the V plane

Figures 12 and 13 show CT scans of sample III in the H and V planes, respectively. The material is almost homogeneous, meaning there is no significant difference between the horizontal and vertical sections. Also, there is no noticeable difference between the matrix and fly ash. Due to the intensive plastic deformation and rotation of the samples, the fly ash is

ultimately well mixed in the matrix, and pores are eliminated. The results are similar to those obtained for the aluminium composite with 4% fly ash [27].

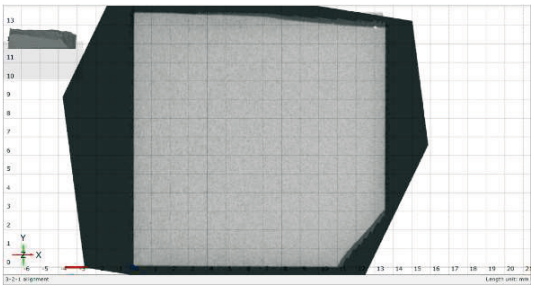

Fig. 12 A CT scan of the sample III in the H plane

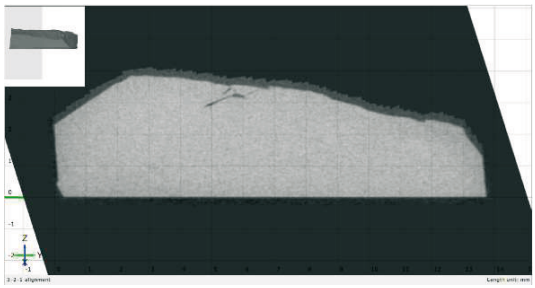

Fig. 13 A CT scan of the sample III in the V plane

It should be noted that with the ECAE process, part of the material had to be cut off after each pass. The reason for that is that in the ECAE process, the friction conditions are not the same in all the parts of the channels. Therefore, some material particles travel faster and others slower, and the sample edges become irregularly shaped and bevelled, and they need to be cut off before the next pass [24,26,27]. Also, the ECAE parameters were kept the same for all passes to ensure equal experimental conditions. As this specific combination of the A356 alloy and fly ash, originating from Serbia, is a novelty of this research, the chosen parameters are not the optimal ones. Because of that, some pieces broke in the third pass due to severe plastic deformation. This is visible in Figure 13 as an irregular shape, along with some surface cracks. Optimisation of ECAE parameters may be the subject of subsequent research.

3.4 Vickers hardness

Figure 14 shows the results of the HV1 hardness measurement, which was conducted at a test load of F = 9.81 N. The mean value of the measurement results was obtained as the arithmetic mean of 12 repetitions. All measurements were made on a cross-section of the sample perpendicular to the extrusion direction.

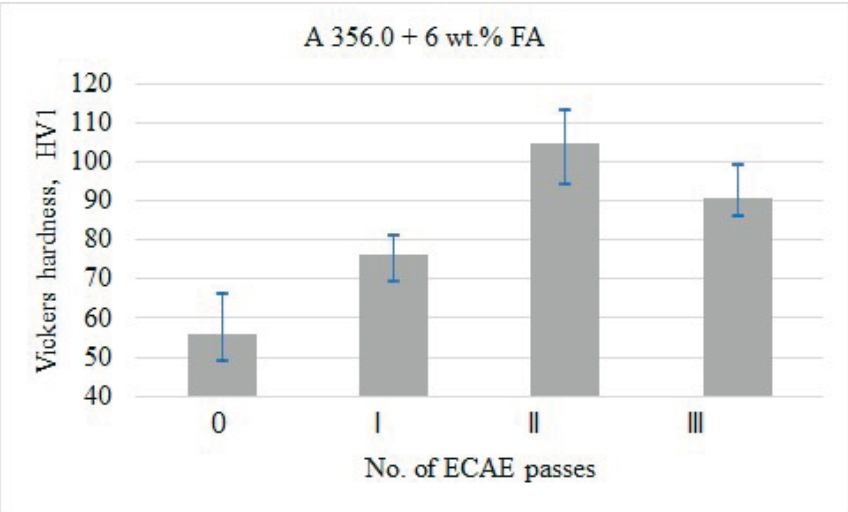

Fig. 14 Influence of the deformation degree on the Vickers hardness of the composite

In Figure 14, the blue colour shows the measurement dissipations as well as both the maximum and minimum values. The standard deviations of the measurements were SD_0 = 5, SD_I = 3, SD_{II} = 6, and SD_{III} = 4. In general, the minimum measured value was 49 HV1 for the cast composite sample, and the maximum was 113 HV1 for the two-time extruded composite.

After the first pass, the mean hardness value increased from 56 HV to 76 HV, i.e., by 35.7%. After the second pass, the mean hardness value increased from 76 HV to 105 HV, representing a 38.7% increase. The maximum increase in the mean hardness value HV1 of the sample after two ECAE passes compared to the cast sample is 87.5%. Similar trends have recently been reported by various researchers in the studies [21-23] and also in the studies [26,27].

The three-time extruded composite shows a decrease in hardness compared to the twice-extruded sample. This result is unexpected, considering the refinement of the microstructure, but this is likely due to the appearance of cracks caused by severe plastic deformation. Some of these cracks are visible in the SEM images shown in Figures 15a and b. The scans were taken with a Tescan Vega TS5136MM SEM (TESCAN, Brno, Czech Republic). Figure 15a shows the sample number III under a magnification of 500×, where several cracks are visible, while Figure 15b shows the same sample with a focus on one crack that spreads across the scan. The image in Figure 15b has the maximum magnification, exceeding 3000×, that can be achieved with the device. Although the focus in this figure was on the appearance of the crack, microscopic fly ash particles are also visible, nicely embedded within the matrix.

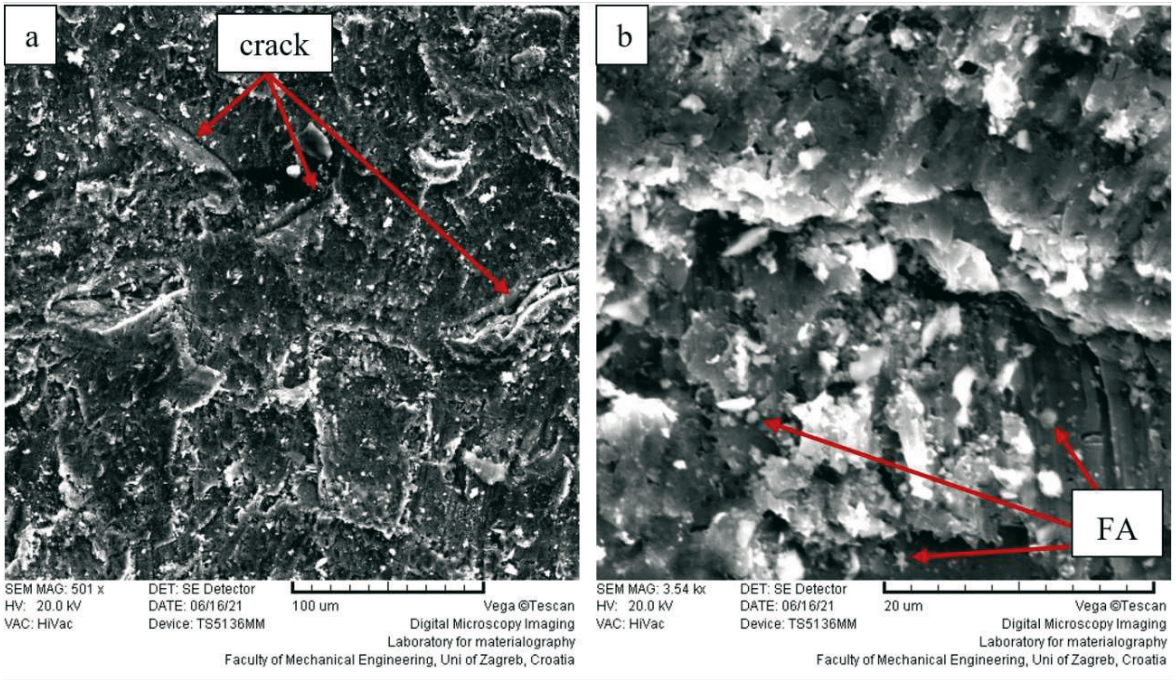

Fig. 15 SEM scans of the sample III: a) at magnification 500×, b) at magnification 3000×

Given that this sample was partially broken, it can be concluded that for the specific parameters used, the best HV1 results were obtained with two ECAE passes. This also confirms that optimisation of ECAE parameters is necessary, which sets a clear direction for future research.

4. Conclusions

Based on the conducted research and the obtained results, the following conclusions can be drawn:

- Using the compo casting method, a composite based on the A356 alloy with 6wt.% fly ash (FA) as reinforcement can be produced. Analysis with an optical microscope shows that this composite has a non-dendritic microstructure, while CT scans reveal well-distributed fly ash in both the horizontal and vertical cross-sections.

- Equal channel angular extrusion (ECAE) improves the microstructure of the composite. The grain size is reduced by 65%, and fly ash is even better distributed in the matrix. Silicon particles are broken due to intense shear forces. Pores, visible on the CT scan of the cast sample, are eliminated after extrusion.
- Due to the structure development, according to the Hall-Petch equation, strengthening of the material of at least 3.2–7% is expected, and the Vickers hardness is increased by 87.5% after two ECAE passes.
- The Vickers hardness decreases after the third ECAE pass due to the cracks observed on the SEM scan. Cracks and breaks are caused by severe plastic deformation, indicating the necessity of optimising the ECAE parameters.

There are several potential areas for future research. One area involves the development of technology for the preparation of aluminium-fly ash composites, focusing on the use of various matrix materials while maximising the fly ash content. The other important area is the optimisation of ECAE parameters to achieve the most refined and uniform microstructure with the minimum number of passes. Additionally, the effects of elevated temperatures and the application of back pressure during the ECAE process require further investigation. It is also essential to conduct comprehensive studies on the other properties of this specific composite, such as fatigue behaviour, tensile strength, and wear resistance.

Acknowledgment

This research was partially supported by the Federal Ministry of Education and Science, Bosnia and Herzegovina.

REFERENCES

[1] Parikh, V.K.; Patel, V.; Pandya, D.P.; Andersson, J. Current Status on Manufacturing Routes to Produce Metal Matrix Composites: *State-of-the-Art. Heliyon* **2023**, 9. https://doi.org/10.1016/j.heliyon.2023.e13558

[2] Dwivedi, S.P.; Sharma, S.; Mishra, K.R. A356 Aluminum Alloy and Applications- A Review. *International Journal of Advanced Materials Manufacturing & Characterization* **2014**, 4, 81–86. https://doi.org/10.11127/ijammc.2014.08.01

[3] Mussatto, A.; Ahad, I.U.I.; Mousavian, R.T.; Delaure, Y.; Brabazon, D. Advanced Production Routes for Metal Matrix Composites. *Engineering Reports* **2021**, 3. https://doi.org/10.1002/eng2.12330

[4] Verma, V.; Khvan, A. A Short Review on Al MMC with Reinforcement Addition Effect on Their Mechanical and Wear Behaviour; **2019**. https://doi.org/10.5772/intechopen.83584

[5] Kasar, A.K.; Gupta, N.; Rohatgi, P.K.; Menezes, P.L. A Brief Review of Fly Ash as Reinforcement for Composites with Improved Mechanical and Tribological Properties. *JOM* **2020**, 72, 2340–2351. https://doi.org/10.1007/s11837-020-04170-z

[6] Mathapati, M.; Amate, K.; Durga Prasad, C.; Jayavardhana, M.L.; Hemanth Raju, T. A Review on Fly Ash Utilization. *Mater Today Proc* **2022**, 50, 1535–1540. https://doi.org/10.1016/j.matpr.2021.09.106

[7] Ghazali, N.; Muthusamy, K.; Wan Ahmad, S. Utilization of Fly Ash in Construction. *IOP Conf Ser Mater Sci Eng* **2019**, 601, 012023. https://doi.org/10.1088/1757-899X/601/1/012023

[8] Choudhury, A.; Nanda, J.; Das, S.N. Enactment of Aluminium-Fly Ash Composites. *J Phys Conf Ser* **2020**, 1706, 012138. https://doi.org/10.1088/1742-6596/1706/1/012138

[9] Ramanathan, A.; Krishnan, P.K.; Muraliraja, R. A Review on the Production of Metal Matrix Composites through Stir Casting – Furnace Design, Properties, Challenges, and Research Opportunities. *J Manuf Process* **2019**, 42, 213–245. https://doi.org/10.1016/j.jmapro.2019.04.017

[10] Pola, A.; Tocci, M.; Kapranos, P. Microstructure and Properties of Semi-Solid Aluminum Alloys: A Literature Review. *Metals (Basel)* **2018**, 8, 181. https://doi.org/10.3390/met8030181

[11] Maksimović, V.M.; Devečerski, A.B.; Došen, A.; Bobić, I.; Erić, M.D.; Volkov-Husović, T. Comparative Study on Cavitation Erosion Resistance of A356 Alloy and A356FA5 Composite. *Transactions of the Indian Institute of Metals* **2017**, 70, 97–105. https://doi.org/10.1007/s12666-016-0864-1

[12] Sharma, A.K.; Bhandari, R.; Pinca-Bretotean, C. A Systematic Overview on Fabrication Aspects and Methods of Aluminum Metal Matrix Composites. *Mater Today Proc* **2021**, 45, 4133–4138. https://doi.org/10.1016/j.matpr.2020.11.899

[13] Kar, A.; Sharma, A.; Kumar, S. A Critical Review on Recent Advancements in Aluminium-Based Metal Matrix Composites. *Crystals (Basel)* **2024**, 14, 412. https://doi.org/10.3390/cryst14050412

[14] Thangaraju, S.; Heilmaier, M.; Murty, B.S.; Vadlamani, S.S. On the Estimation of True Hall–Petch Constants and Their Role on the Superposition Law Exponent in Al Alloys. *Adv Eng Mater* **2012**, 14, 892–897. https://doi.org/10.1002/adem.201200114

[15] Maddaiah, K.C.; Kumar, G.B.V.; Pramod, R. Studies on the Mechanical, Strengthening Mechanisms and Tribological Characteristics of AA7150-Al2O3 Nano-Metal Matrix Composites. *Journal of Composites Science* **2024**, 8, 97. https://doi.org/10.3390/jcs8030097

[16] Segal, V. Equal-Channel Angular Extrusion (ECAE): From a Laboratory Curiosity to an Industrial Technology. *Metals (Basel)* **2020**, 10. https://doi.org/10.3390/met10020244

[17] Edalati, K.; Horita, Z. High-Pressure Torsion of Pure Metals: Influence of Atomic Bond Parameters and Stacking Fault Energy on Grain Size and Correlation with Hardness. *Acta Mater* **2011**, 59, 6831–6836. https://doi.org/10.1016/j.actamat.2011.07.046

[18] Salam Abood, A.; P K, J.; Karuna, G.; Jain, A.; Goel, R.; Kumar Chandra, P. Advancing Aluminum-Based Composites with Fly Ash and SiC Reinforcement through Stir Casting. *E3S Web of Conferences* **2024**, 507, 01050. https://doi.org/10.1051/e3sconf/202450701050

[19] Lakshmi Narayana, K.S.; Benal, M.M.; Shivanand, H.K. Effect of Fly Ash on Aluminum Matrix Composites Produced by Stir Casting Route: A Review. *Journal of Emerging Technologies and Innovative Research (JETIR)* **2019**, 6, 489–499.

[20] Zhang, X.; Han, J.; Tian, J.; Zhu, L.; Zhang, P.; Wang, Y.; Jiang, Z. The Effects of Pass Number and Die Channel Angle of Equal Channel Angular Pressing on Innovative Magnesium Composite Material. *Metals (Basel)* **2025**, 15, 349. https://doi.org/10.3390/met15040349

[21] Kunčická, L.; Kocich, R. Characterizing the Behavior and Microstructure of Cu-La2O3 Composite Processed via Equal Channel Angular Pressing. *Metals (Basel)* **2025**, 15, 368. https://doi.org/10.3390/met15040368

[22] Liu, Y.; Xu, J.; Chen, B.; Fan, Y.; Lv, W.; Sun, H. The Influence of Equal-Channel Angular Pressing on the Microstructure and Properties of a Steel–Aluminum Composite. *Metals (Basel)* **2025**, 15, 774. https://doi.org/10.3390/met15070774

[23] Berndt, N.; Reiser, N.A.; Wagner, M.F.-X. Evolution of Plastic Deformation during Multi-Pass ECAP of an AA6060 Aluminum Alloy – An Experimental Flow Line Analysis. *Journal of Materials Research and Technology* **2025**, 34, 359–371. https://doi.org/10.1016/j.jmrt.2024.12.048

[24] Muslić, M.; Rede, V.; Maksimović, V. Solid Particle Erosion Resistance of al Alloy and al Alloy-Fly Ash Composite Subjected to Equal-Channel Angular Pressing. *Metallurgical and Materials Engineering* **2021**, 27, 15–26. https://doi.org/10.30544/624

[25] Muslić, M.; Maksimović, V.; Bobić, I. Casting an Al Alloy 2024 + 4% Fly Ash Composite Suitable for Processing by Plastic Deformation. *In Proceedings of the Proceedings Book of the 17th International Foundrymen Conference*, Hi-Tech Casting Solution and Knowledge Based Engineering; Dolić, N., Zovko Brodarac, Z., Begić Hadžipašić, A., Eds.; Metalurgical faculty, University of Zagreb, Croatia: Opatija, May 16 2018; pp. 364–371.

[26] Muslić, M.; Orešković, L.; Rede, V.; Maksimović, V. Indentation Size Effect of Composite A356 + 6%FA Subjected to ECAP. *Metals (Basel)* **2022**, 12, 821. https://doi.org/10.3390/met12050821

[27] Muslić, M.; Rede, V.; Maksimović, V.; Ćorić, D. Hardness and Microstructural Characterization of Al/FA Composites Fabricated by Compo Casting and the Equal Channel Angular Extrusion. *Processes* **2025**, 13, 928. https://doi.org/10.3390/pr13040928

[28] Filetin, T.; Kovačiček, F.; Indorf, J. Svojstva i Primjena Materijala / Properties and Application of Materials; Pustaić, D., Ed.; 7th ed.; Faculty of Mechanical and Naval Engineering, University of Zagreb: Zagreb, **2002**; Vol. 1.

[29] Malaki, M.; Tehrani, A.F.; Niroumand, B.; Gupta, M. Wettability in Metal Matrix Composites. *Metals (Basel)* **2021**, 11. https://doi.org/10.3390/met11071034

[30] Skrotzki, W. Deformation Heterogeneities in Equal Channel Angular Pressing. *Mater Trans* **2019**, 60, 1331–1343. https://doi.org/10.2320/matertrans.MF201926

[31] ASTM E112-24 - Standard Test Methods for Determining Average Grain Size, **2024**.

[32] https://www.modulusmetal.com/Aluminum-356-0-vs-A356-0-Sand-Cast-T6

Submitted: 12.5.2025

Accepted: 07.9.2025

Merima Muslić*
E-PRO Ltd. for Design, Engineering, and Technical Consulting, Bihać, Bosnia and Herzegovina
Vera Rede
Zdenka Keran
Helena Lukšić
University of Zagreb, Faculty of Mechanical Engineering and Naval Architecture, Zagreb, Croatia
*Corresponding author:
dmuslic@bih.net.ba